Middle-East Journal of Scientific Research 14 (10): 1345-1353, 2013
ISSN 1990-9233

DOI: 10.5829/idosi.mejsr.2013.14.10.2338

Effect of Height on the Seismic Behavior of Reinforced Concrete Bearing Wall Structural Systems with High Ductility

[1]Yousef Zandi, [2]Maedeh Sadeghi, [3]Abouzar Jafari and [4]Ali Keyhani

[1]Civil Engineering Department, Tabriz Branch, Islamic Azad University, Tabriz , Iran
[2]Mirdamad University of Gorgan, Gorgan, Iran
[3]Sistan and Baluchestan University, Zahedan, Iran
[4]Civil Engineering Faculty, Shahrood University of Technology, Shahrood, Iran

Abstract: Investigation on the effect of the height as an influencing parameter on the seismic performance of reinforced concrete bearing wall structures with high ductility is the subject of this article. For this purpose, a few models with different heights but similar planar layout of walls are taken into consideration. In this research the nonlinear behavior of the models is studied by employing the finite element method for multi-layer shells with fiber sections together with the potential formation of plastic hinges where the mechanical properties of various steel and concrete fibers are taken into account. Carrying out the nonlinear analyses, some seismic parameters such as dominant structural vibration modes, ductility coefficients, the strength factor and response modification factor are evaluated. The obtained results indicate a satisfactory seismic behavior with a prevailing torsional mode for the studied models when their heights are within the allowable range. However, common use of these systems requires a more thorough investigation.

Key words: Seismic rehabilitation % Bearing wall system % High ductility % Response modification factor

INTRODUCTION

Using concrete slab-wall structures with high ductility as lateral loads resisting systems for tall and special buildings seems a plausible policy in Earthquake-prone countries because of their satisfactory seismic behavior in previous earthquakes. Relatively higher structural integrity, low thickness of walls, limited construction details needed to provide ductile behavior and three-dimensional behavior of walls because of interconnections between perpendicular walls can be mentioned as some of the advantageous factors of this system [1]. Openings in structural walls are common and usually inevitable due to functional requirements that needs a great deal of attention because of the relatively low thickness of coupling beams and having considerable shear due to the coupling of walls functioning with large forces [2]. Also, in this system, yield of bending rebars in plastic hinge, which occurs in the bottom of the wall, controls strength, non-elastic deformation and energy waste. In other words, in order to raise ductility, the concrete placed in compressive area of shear wall should not be crushed before yielding of longitudinal reinforcements. Confining the concrete inside a shear wall via transversal reinforcements increases compressive strain of concrete significantly and results in delayed compressive failure of the concrete. This will cause to form plastic hinge at the end of the wall before failure and helps having a ductile behavior [3].

Several authors have worked on concrete slab and wall systems focusing on the performance level of the systems with low and intermediate ductility [4, 5] and study of seismic behavior and response modification factor of the systems [6-8]. However, the study on the effect of high ductility has rarely been taken in to consideration. Therefore, it seems plausible to about the seismic behavior of systems with a high level of ductility. In the present study, to evaluate some important seismic parameters and seismic behavior of concrete slab-wall structures with high ductility, five three-dimensional structural models with different heights but similar planar layouts are taken into consideration. The plans are symmetrical in both directions and comprise combination of cross-shaped, T-shaped and L-shaped walls that are chosen due to different deformation capacities of the shapes in each direction.

Corresoinding Author: Yousef Zandi, Civil Engineering Department, Tabriz Branch, Islamic Azad University, Tabriz , Iran. E-mail: zandi@iaut.ac.ir.

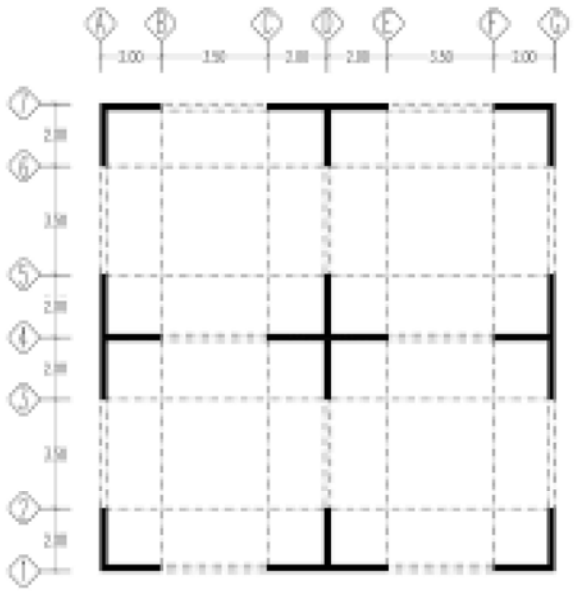

Fig. 1: Plan of the models

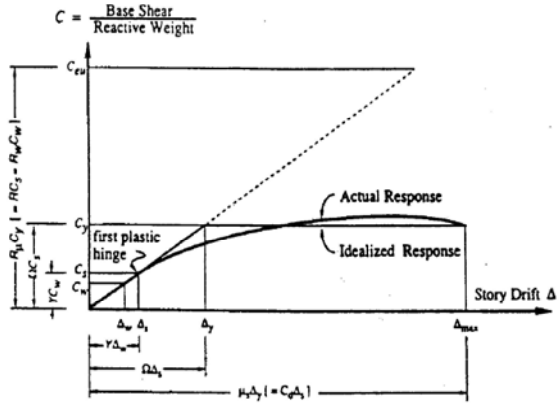

Fig. 2: Overall response of the structure (Basic shear coefficient -story Drift).

The Studied Models: All the models were chosen to be symmetrical with a length of 15 m in both directions which were formed through a combination of cross-shaped, T-shaped and L-shaped walls. In designing the models, the structural system was regarded as a combinations of reinforced concrete shear walls with high ductility to resist the lateral loads. Coupling beams in all the models have 120 cm height in both directions. In all models, the opening widths were the same in both H_2 and H_1 directions (Fig. 1). Structure design was performed using ETABS 9.20 Software. The studied structures were analyzed and designed according to the Iranian Seismic Code (ISC) [9] and the ACI 318-99 [10]. The models heights were as follows:

- 4S: the first model with 4 story and 13.20 m high;
- 8S: the second model with 8 story and 26.40 m high;
- 12S: the third model with 12 story and 39.60 m high;
- 16S: the forth model with 16 story and 52.80 m high;
- 20S: the fifth model with 20 story and 66.00 m high.

Evaluation of Response Modification Factor: Response modification factor of structures depends on several parameters and determination of the factor is very complicated. The factor is different for two structures with a same structural system with different periods and even with a same period and different design. So, using a fixed factor for a structural system without considering the mentioned criteria may not be correct. The overall and ideal behavior of the structure gradually increase under static loading (Fig. 2) [11].

On this basis, the needed elastic strength with basic shear coefficient (C_{eu}) is given as Equation 1

$$C_{\text{eu}} = \frac{V_e}{W} \tag{1}$$

where W and V_e are the stationary weight of the structure and the maximum base shear in the structure in elastic level, respectively. Due to ductility in real structures, an economical structure can be designed to have the maximum $C_y.W$ where the maximum drift of the structure is defined as $D_{\max}$. $D_{\max}$ is related to the load that the structure can bear considerably without losing its strength. Dy is the Drift of the structure at the yielding threshold. Ductility in the structure is defined as Equation 2:

$$\mu = \frac{\Delta_{\max}}{\Delta_y} \tag{2}$$

Due to ductility, the structure is prone to lose hysteresis energy. Therefore, elastic force of the structure (V_e) can be decreased via a coefficient called ductility coefficients (R_μ) according to Equation 3:

$$R_\mu = \frac{C_{eu}.W}{C_y.W} = \frac{C_{eu}}{C_y} \tag{3}$$

In this equation, Cy is a force in the level of yield of the structure. The stored strength in the structure between real yielding of the structure (Cy) and the first noticeable yielding (Cs) is called the strength factor of the structure which is obtained from Equation 4:

$$R_s = \frac{C_y}{C_s} \tag{4}$$

Considering Fig. 2, total amount of response modification factor related to allowable stress design is obtained through Equation 5:

$$R = \frac{C_{eu}}{C_w} = \frac{C_{eu}}{C_y} \times \frac{C_y}{C_s} \times \frac{C_s}{C_w} = R_\mu \times R_s \times Y \tag{5}$$

Y is called allowable stress factor which is approximately between 1.4 and 1.5 in different codes of practice.

Therefore, the main parameters affecting response modification factor are ductility coefficients (Rμ) and the strength factor (Rs). It should be noted about ductility coefficients (Rμ) that structures dissipate a great amount of seismic energy as hysteresis depending on the overall ductility of the structure. The overall ductility should be such that the local ductility of members does not exceed allowable limit. To reach this aim, the minimum needed strength of the structure, which limits its overall ductility to a predefined ductility level, should be determined. In order to estimate the ductility coefficient (Rμ), Krawinkler and Nassar [12] and Newmark and Hall [13], methods were adopted in the present study.

Modeling of Nonlinear Behavior: In order to model the nonlinear behavior of shear walls and coupling beams, FEMA 273 [14] was used. According to the guideline, the walls are slender in both directions and their nonlinear behavior is controlled by flexure. To obtain a more realistic estimation for behavior of the considered models, instead of the commonly practiced equivalent beam-column models, here a finite element model with multi-layered shell elements is employed that is able to take into account the cracking of the concrete and consequently shifting of the neutral axis of the flexural members. In order to define the cross section of each layer in the PERFORM 3D [15] software, the so named fiber sections are used. By using these fiber sections the cross sections of elements are described and a non-linear behavior modeling is constructed. Modeling of the cross section of each element should be done by an adequate arrangement of steel and concrete fibers. The behavior of the fibers has been defined using the stress-strain curves with a high level of accuracy. Each element, which is considered as a layer, describes one of the mechanical characteristics of reinforced concrete. To model the behavior of concrete shear walls, several layers are employed which are joined

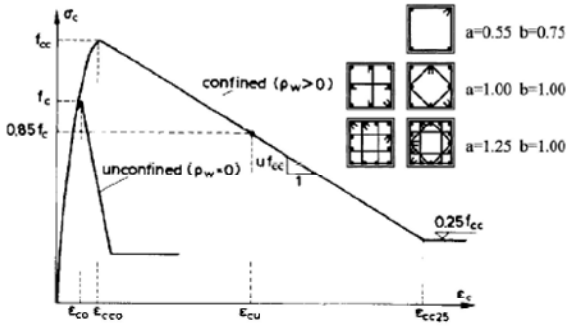

Fig. 3: Mono-axial stress-strain curves for concrete fibers

in a parallel fashion. To model nonlinear behavior of slender walls among available elements in the software library, the shear wall element' is employed. Combination of the two axial-bending and shear layers models flexure and shear behavior in these walls. These layers are joined in the nodes of elements and behave as parallel layers. In this research three kinds of layers have been employed including:

- The concrete axial-bending layer
- The steel axial-bending layer
- The concrete shear layer

Properties of Concrete and Steel Fibers: Kappos [16] presented stress-strain relationship for confined and non-confined concretes (Fig. 3). According to his suggested model, mono-axial stress-strain curve of concrete is made up of two parts: the rising branch to maximum pressure strength which is defined as Equation 6 where f_c and ε_{co} are compressive strength of non-confined concrete and strain rate in maximum compressive stress of non-confined concrete, respectively; and the descending branch of strain softening is a straight line which declines with u rate per strain unit (Equation 7). In the equation, f_{cc}, ρ_w, b_c, s_w, k and ε_{cco} are compressive strength of confined concrete, volumetric ratio of hoop reinforcement, the width of the confined core, the hoop spacing, confining index which is obtained through Equation 8 and strain in maximum compressive stress of confined concrete, respectively.

$$\sigma_c = f_c \left[2\left(\frac{\varepsilon_c}{\varepsilon_{c0}}\right) - \left(\frac{\varepsilon_c}{\varepsilon_{c0}}\right)^2 \right] \tag{6}$$

$$u = \frac{0.5 f_{cc}}{0.75\rho_w \sqrt{b_c / s_w} + \frac{3 + 0.29 f_c / k}{145 f_c / k - 1000}} - \varepsilon_{cco} \tag{7}$$

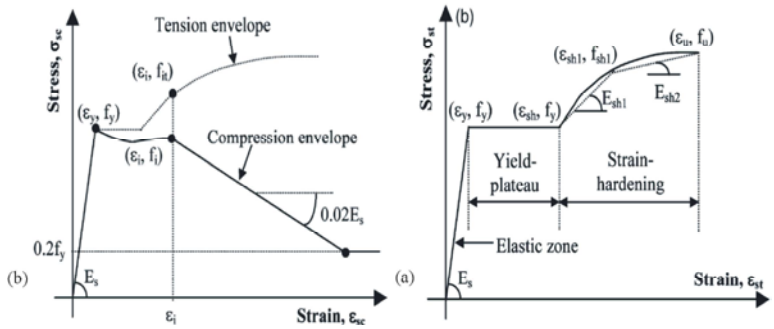

Fig. 4: Mono-axial stress-strain curves for steel fibers in only tension part (a) and only compression part (b).

$$k = 1 + a(\rho_w \frac{f_y}{f_c})^b \quad (8)$$

Amount of k is basically related to ρ_w, f_y (yield strength of lateral steels) and f_c (compressive strength of non-confined concrete). Experimental ratios of a and b are functions of amount of hoop reinforcement (Fig. 3). For modeling the cracking phenomenon in wall sections considering the points which have high cracking potential, i.e. wall edges, the area of the fibers in these points are considered much more smaller than other points. Therefore, the fibers which are located on the edges of these walls rupture sooner. As a result, cracking phenomenon and shifting of the neutral axis are being modeled with high accuracy. Also, concrete and steel bending-axial layers are both for modeling bending and axial behaviors and fibers of these layers are solely in the direction of wall height. In other two directions (i.e. wall width and out-of-plane), the section is considered to be elastic.

For modeling steel reinforcement, buckling steel fibers and non-buckling steel fibers are adopted. In boundary zone where distance of confining stirrups reach an amount that longitudinal reinforcement cannot be buckled, non-buckling steel fibers are used, while in other parts, buckling steel fibers are adopted. In buckling steel fibers, stress-strain curves of tension and compression parts are shown in Fig. 4 (a)[17] and (b)[18], respectively. For non- buckling steel fibers, stress-strain curves of tension and compression parts are same (Fig. 4 (a)).

The Concrete Shear Layer: The third layer which is used for modeling the wall elements is called the concrete shear layer. The fibers are not used in constructing such a wall. This layer is used for modeling shear behavior in concrete; shear behavior in walls is considered to be nonlinear in the present study [19]. To make this layer, shear modulus (G) and shear strength of concrete (v_c) are used. To determine shear capacity of shear layer according to FEMA 272, the methods in ACI 318-99 were used and shear strength of concrete of the layer is considered to be between 19.16 and 15.16 kg/cm^2 in terms of relative parameters. To determine shear modulus, if $v = 0.25$, shear modulus is 0.4 E. For concrete materials in non-cracked form, the stress is used until 0.5 Vn, while for cracked form, shear module of nonlinear part is regarded to be 0.25 of shear module of elastic status and equivalent strain of yield point of shear materials of the layer is hypnotized to be 0.004 [20].

Nonlinear Modeling in Coupling Beams: For modeling nonlinear behavior in these beams, both possible nonlinear behaviors (i.e. bending and shear nonlinear behaviors) are considered. In modeling bending behavior, 'FEMA beam element' are used instead of plastic hinges. The base in these elements is chord rotation model (Fig. 5 (a)). The key in this model is that force-deformation relation is like rotating moment of end of the member versus rotation of end of the member. Considering Fig. 5 (b) which indicates, moment of end of the member versus rotation of the member, it can be seen that primary stiffness of beam considering its inflection point, in middle of the member, is 6EI/L and after that, behavior is nonlinear. In this model, it is hypothesized that the inflection point is in the middle. For more accurate estimation of behavior of coupling beams along the beam, two elements of FEMA beam is used because of possibility of having different end moments. Also, the location of the inflection point can be considered to be somewhere other than the middle. In 'FEMA beam element', deformation capacity is defined as chord rotation. For modeling bending nonlinear behavior in coupling beams, the tables and obligations provided in FEMA guideline [14] were used [15].

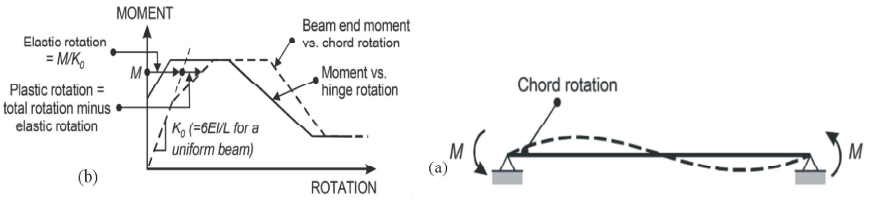

Fig. 5: Chord rotation model(a)and beam end moment vs chord rotation in member rotation model (b)

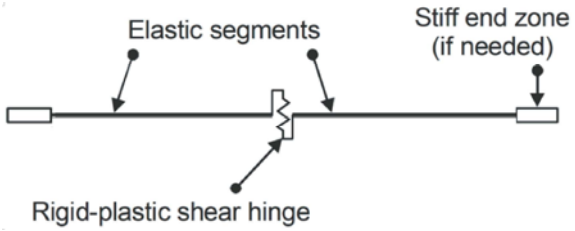

Fig. 6: Rigid plastic shear hinge model. [15]

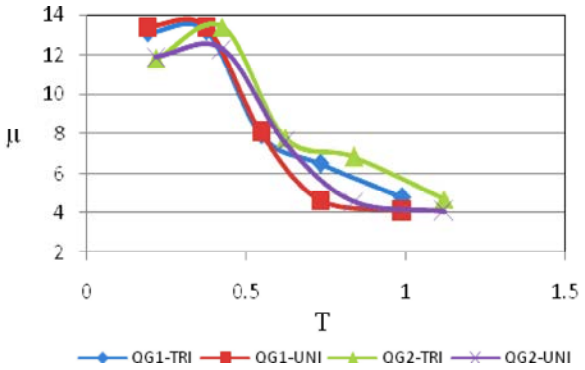

Fig. 7: Variations of ductility ratio versus period.

For modeling shear nonlinear behavior, 'rigid plastic shear hinges' are used (Fig. 6). In these hinges, deformation parameter along shear hinge is used for modeling deformation capacity of the hinge. For modeling shear nonlinear behavior, FEMA 273 was used; however, the relationship between nominal strength and rotation uses a bilinear relation to nominal shear strength instead of the presented figure in this guideline where a linear relation to nominal shear strength (Vn) is used. The relation between shear force versus rotation in first part with infinite slope reaches a shear with half nominal shear strength which is defined considering the ACI 318-99 and then, it reaches nominal shear strength (Vn) in a rotation of 0.004 [15].

Numerical Analyses: After nonlinear modeling, the models are analyzed. In the present study, two types of analyses were utilized, i.e. linear dynamic analysis and nonlinear static analysis. Linear dynamic analysis is used for estimation of modes and period of each one and nonlinear static analysis is adopted to estimate seismic parameters such as the ratios of ductility, ductility coefficient, the strength factor and response modification factor. After performing nonlinear static analyses, base shear- reference drift curves of a point of the roof (in the present study, the mass center of the roof is considered) is obtained. The analyses are controlled by drift types so that with uniform increase in drift, increased force to make that drift is estimated and the force is imposed to the structure. To choose lateral loads distribution pattern, in FEMA 273 were used:

- TRI (Triangular lateral load pattern)
- UNI (Uniform lateral load pattern)

Also, for gravitational loading in every analysis, according to FEMA 273, gravitational loads are driven as lower and upper bounds of gravitational loads which are shown as Q_{G1} and Q_{G2}, respectively and are estimated through the Equations 9 and 10, respectively:

$$Q_{G1} = 0.9Q_D \quad (9)$$

$$Q_{G2} = 1.1(Q_D + Q_l) \quad (10)$$

After performing the mentioned analyses for all the samples, surveying on push-over curves and important seismic parameters are done, such as period and shape of the modes, the ratios of ductility (μ), ductility coefficient (Rμ), the strength factor (Rs) and response modification factor (R), are estimated so that seismic behavior of these structural systems is accurately determined using the data.

Survey of the Results Obtained from the Analyses: Considering Fig. 7, a same trend can be detected in variations of ductility ratios in both gravitational load patterns and both lateral load distribution patterns. As period increases, ductility of the structure decreases. Also, it can be seen that ductility ratio of 8S model, as compared to 4S, is higher, which seems to be logical

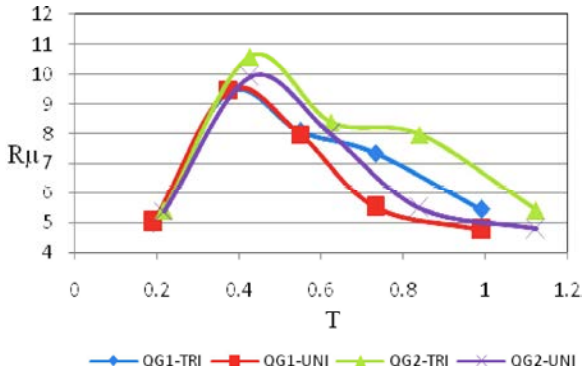

Fig. 8: Variations of ductility coefficient versus period.

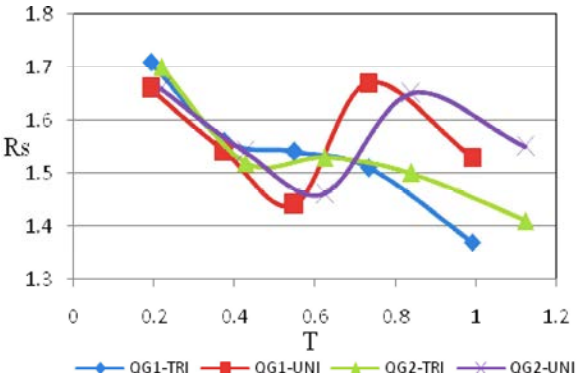

Fig. 9: Variations of strength factor versus period.

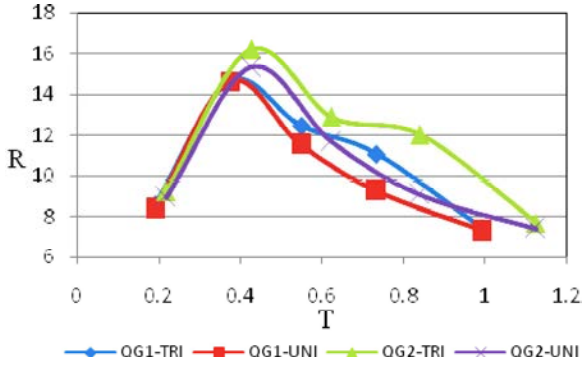

Figg. 10: Variations of response modification factor versus period.

considering low height of the sample and its brittle behavior. descending trend of ductility ratio shows that with increases height and clear bending behavior in samples, ductility ratio starts to decrease and therefore, it can be concluded that the higher the heights of samples especially higher than allowable height mentioned in the Iranian Seismic Code (ISC), the smaller ductility ratio and nearer reference drift of the mechanism point of the structure and reference drift of yield point. Thus, the structural system in this range of height shows a brittle behavior. By comparing gravitational loading patterns in each model, it can be understood that higher bound of gravitational loading shows a higher ductility ratio than lower bound of gravitational loading. Also, by comparing lateral loading patterns for each model, it can be seen that triangular load pattern obtains higher ductility than uniform load pattern.

A rather same trend is seen in Fig. 8 which is consistent with variations of ductility ratio. This looks logical as ductility coefficient is directly related to ductility ratio. By comparing gravitational loading patterns in each model, higher bound of gravitational load has higher ductility coefficient than that of lower bound of gravitational load. Also, by comparing lateral loading models in each model, it can be seen that triangular load model has higher ductility coefficient than that of uniform load model.

A different trend is seen in Fig. 9. In this figure, the highest and lowest strength factor are for 4S and 20S models, respectively, while these parameters is same in other samples. The most obvious result is low effect of height on strength factor. The coefficient is higher in low height and rigid structures with lower ductility and period and it doesn't show much sensitivity to increased height. It should be noted that 4S model has a high structure design which results in higher strength factor in this sample. Although it is expected that strength factor of 20S is same as the three preceding samples, this model has higher strength factor with higher height. The reason can be found in very strong structure and bending behavior in this model. Although the model has a high strength factor, the model reaches its maximum strength in a small drift due to low ductility ratio; this behavioral non-ductile cracking looks to be unfavorable.

Considering Fig.10 and comparing gravitational loading patterns in each model, higher bound of gravitational loading has a higher response modification factor than lower bound of gravitational loading. Also, by comparing lateral loading patterns in each model, it can be seen that triangular load pattern has higher response modification factor than uniform load pattern. It can be seen that response modification factor variations trend is rather similar to ductility coefficient variations trend and this clearly shows that effect of strength factor on response modification factor is very low and ductility coefficient has a considerable role in amount of response modification factor. In this figure, the highest and lowest response modification factor is for 8S and 20S, respectively. The figure shows that response modification factor decreases with increased ductility coefficient so

Table 1: Period and type of first modes in samples

Model	T(s)	Shape of first mode
4S-QG1-TRI	0.1917	transitional
4S-QG1-UNI	0.1917	transitional
4S-QG2-TRI	0.2187	transitional
4S-QG2-UNI	0.2187	transitional
8S-QG1-TRI	0.3751	torsional
8S-QG1-UNI	0.3751	torsional
8S-QG2-TRI	0.4273	torsional
8S-QG2-UNI	0.4273	torsional
12S-QG1-TRI	0.5487	torsional
12S-QG1-UNI	0.5487	torsional
12S-QG2-TRI	0.6236	torsional
12S-QG2-UNI	0.6236	torsional
16S-QG1-TRI	0.7326	torsional
16S-QG1-UNI	0.7326	torsional
16S-QG2-TRI	0.8391	torsional
16S-QG2-UNI	0.8391	torsional
20S-QG1-TRI	0.9907	torsional
20S-QG1-UNI	0.9907	torsional
20S-QG2-TRI	1.123	torsional
20S-QG2-UNI	1.123	torsional

that the amount is higher than the allowable amount of the Iranian Seismic Code (ISC) and lower than the mentioned behavior coefficient in this standard. This can be one of the reasons for presenting this height as an allowable height of this structural system in the ductility range.

As it can be seen from Table 1, the first mode of the structure was transitional only in 4S model with 13 m as height, while in other models, the first mode of structures is torsional. Torsional mode in other 4 models shows, considering proper symmetry and distribution of walls in both directions in all samples, the samples have low torsional rigidity and their design will lead to inefficient and insecure structural design only if driving seismic force along two horizontal and perpendicular directions is considered. It can be seen from Table 1 that period in models varies between 0.1917 and 1.123 sec and with increased floors, period of the structure increases. Also, period for higher bound of gravitational loading (Q_{G2}) is higher than that of lower bound of gravitational loading (Q_{G1}).

By comparing figures 11-14, it can be understood that gravitational load pattern of higher bound shows a lower basic shear coefficient along the curve, especially where strength starts to fall. Also, it can be seen that basic shear coefficient for uniform loading pattern is higher than that of triangular load pattern. Base shear coefficient decreases with increased height. However, 4S model has a considerable higher base shear coefficient than other models. This can be due to meeting the minimum designing requirements of codes in the ductility range so

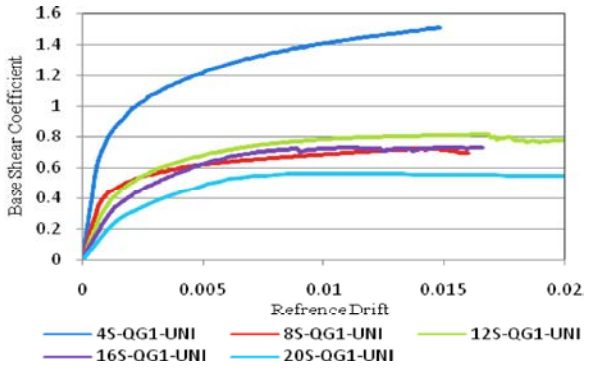

Fig. 11: Pushover curves in gravitational load Q_{G1} and loading pattern UNI

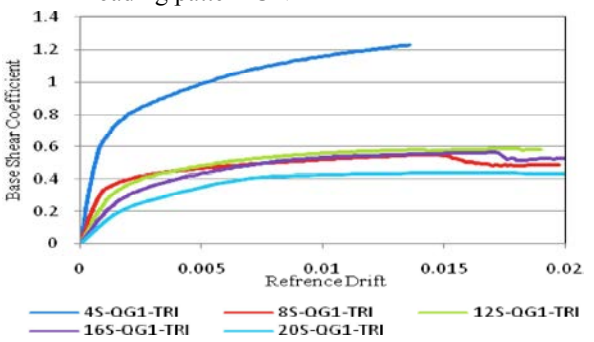

Fig. 12: Pushover curves in gravitational load Q_{G1} and loading pattern TRI

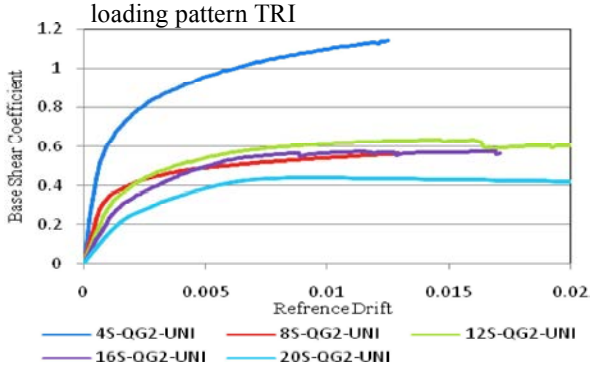

Fig. 13: Pushover curves in gravitational load Q_{G2} and loading pattern UNI

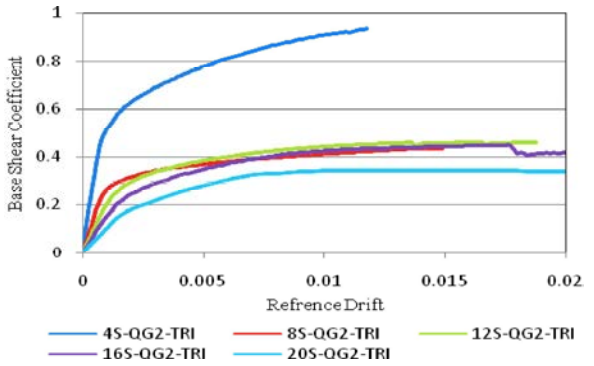

Fig. 14: Pushover curves in gravitational load Q_{G2} and loading pattern TRI

that despite the requirement for minimum amount of resistant elements (percentage of longitudinal and transversal reinforcements, ductility stirrup, etc.), it seems logical that this model has higher strength in terms of its better design. Also, in both gravitational load bound and in all lateral load patterns, 4S curve is very higher than others, while 20S is very lower than other curves. However, curves of other 3 samples are approximately same with overlapping. Lower curve in 20S can be regarded as another reason for considering the mentioned height range in the Iranian Seismic Code (ISC).

CONCLUSION

- Considering properties of the modes, it can be said that the structures have low bending rigidity and their conventional design would lead to an insecure structural design.
- The trend of reduction of the ductility ratio is such that the ratio decreases with increased height and the lowest amount is for 20S model. Also, it can be concluded that the structures show a brittle behavior in an increased height considering plummeted ductility ratio.
- Increased height has a very low influence on strength factor. In lower height and rigid structures with lower ductility and period, the coefficient is higher and doesn't show much sensitivity to increased height.
- Variations of ductility coefficient have a similar trend with ductility ratio and it decreases with increased height. The coefficient is the lowest in the highest model with a height exceeding allowable limit.
- Response modification factor declines with elevated height. Response modification factor of the structures is very sensitive to height variations and designing code cannot provide confidence considering amount of behavior coefficient in an increased height. Higher bound of gravitational loading shows a higher response modification factor than the lower bound. Triangular load pattern obtains a higher behavior coefficient than uniform load pattern.
- Base shear coefficient declines as height increases. However, 4S model has a considerable higher shear coefficient compared to other models.
- According to the obtained results, especially about modes, more detailed investigations with an emphasis on irregular plans with various aspect ratios seems to be necessary in order to find a clear-cut trend in case of secure seismic design for structures.

ACKNOWLEDGEMENT

The authors are grateful to Shahroud University of Technology for financial support.

REFERENCES

1. Balkaya, C. and E. Kalkan, 2004. Seismic vulnerability, behavior and design of tunnel form building structures, Engineering Structures, 26: 2081-2099.
2. Balkaya C a, Kalkan E, 2003, Estimation of fundamental periods of shear-wall dominant building structures, Earthquake Engineering and Structural Dynamics, 32**,** pp 985-998.
3. Greifenhagen, H. and P. Lestuzzi, 2005. Static cyclic tests on lightly reinforced concrete shear walls, Engineering Structures, 27: 1703-1712.
4. Hasani, B. and A. Jafari, 2010. Determination of seismic efficiency of semi-fabricated armed concrete panel structures through nonlinear static and dynamic analyses. International conference on earthquake, university jahad of Kerman Province, Iran.
5. Tehranizadeh, M. and Aziz zadeh Sh, 2009. determination of efficiency level of slab structure and concrete wall designed according to the standard 2800. the fourth conference on designing codes for building against earthquake (standard 2800), Accommodation and Urbanism Organization-Tehran, Iran.
6. Mirghaderi, S., A. Moghaddam and H. Yousefpour, 2009. Determination of nonlinear seismic behavior and behavior coefficient attributes of reinforced concrete structures with application of tunnel molds. the fourth conference on designing codes for building against earthquake, standard 2800, Accommodation and Urbanism Organization-Tehran, Iran.
7. Hasani, B. and A. Jafari, 2008. determination of seismic behavior of reinforced concrete panel structures. Education Technology Journal, Tarbiat Modarres Shahid Rajayee University, third year, third 2: 99-108.
8. Hasani, B. and A. Jafari, 2009. behavior coefficient of reinforced concrete pre-molded panel structures. the fourth conference on designing codes for building against earthquake (standard 2800), Accommodation and Urbanism Organization-Tehran, Iran.
9. Seismic designing code for structures in Iran, 2005. (standard 2800-84 - Iran), investigation center for structures and accommodation, 253-z.

10. American Concrete Institute, ACI 318-99, 1999. Building Code Requirements for Structural Concrete and Commentary - ACI 318R-99, Farming Hills, MI, USA.
11. Uang, C.M., 1991. Establishing R (or Rw) and Cd Factors for Building Seismic Provisions, Journal of Structural Engineering, ASCE, 117(1): 19-28.
12. Krawinkler, H. and A.A. Nassar, 1992. Seismic design based on ductility and cumulative damage demands and capacities, Nonlinear Seismic Analysis and Design of Reinforced Concrete Buildings, Fajfar, Krawinkler.Edd, Elsevier Applied Science, New York.
13. Newmark, N.M. and W.J. Hall, 1982. Earthquake Spectra and Design, Engineering Monograph, Earthquake Engineering Research Institute, Berkeley, California.
14. Federal Emergency Management Agency, FEMA 273,1997, Guideline for the Seismic Rehabilitation of Building, Building Seismic Safety Council, Washington D.C.
15. Computers & Structures, Inc. 2006. PERFORM Components and Elements for PERFORM-3D and PERFORM-COLLAPSE, University Ave.Berkeley, USA.
16. Kappos, A., 1991. Analytical prediction of collapse earthquake for RC buildings: suggested methodology, Earthquake Engineering and Structural Dynamics, 20: 167-176.
17. Dodd, L.L. and J.I. Restrepo-Posada, 1995. Model for predicting cyclic behavior of reinforcing steel, J. Struct Eng, ASCE, 121: 33-45.
18. Monti, G. and C. Nuti, 1992. Nonlinear cyclic behavior of reinforcing bars including buckling, J. Struct. Eng. ASCE, 118: 68-84.
19. Jafari, A., 2008. A Study on the Seismic Behavior of the Panel Structures, MSc Thesis, Shahrood University of Technology.
20. Sadeghi, M., 2011. Effect of height on the Seismic Behavior of Reinforced Concrete Bearing Wall Structural Systems with High Ductility, MSc Thesis, Shahrood University of Technology.